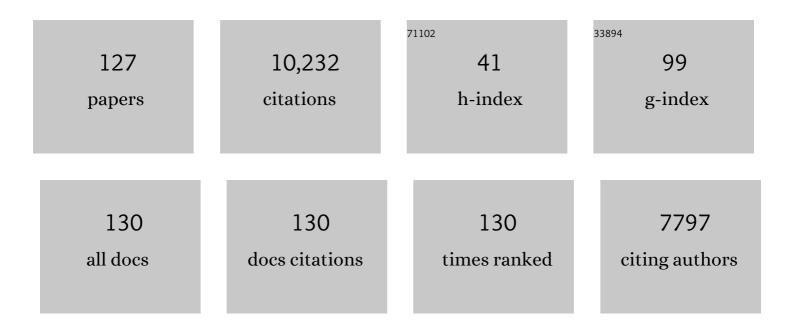
## Henry A Sodano

List of Publications by Year in descending order

Source: https://exaly.com/author-pdf/607339/publications.pdf Version: 2024-02-01



#	Article	IF	CITATIONS
1	Synergetic effect of aramid nanofiberâ€graphene oxide hybrid filler on the properties of rubber compounds for tire tread application. Journal of Applied Polymer Science, 2022, 139, 51856.	2.6	9
2	Enhanced interfacial shear strength in ultra-high molecular weight polyethylene epoxy composites through a zinc oxide nanowire interphase. Composites Science and Technology, 2022, 219, 109218.	7.8	11
3	Aramid Nanofiber Interphase for Enhanced Interfacial Shear Strength in Ultraâ€High Molecular Weight Polyethylene/Epoxy Composites. Advanced Materials Interfaces, 2022, 9, 2102030.	3.7	3
4	Evaluation of Interfacial Shear Strength Healing Efficiency between Dynamic Covalent Bond-Based Epoxy and Functionalized Fiberglass. ACS Applied Polymer Materials, 2022, 4, 2925-2934.	4.4	6
5	Lead titanate nanowires/polyamide-imide piezoelectric nanocomposites for high-temperature energy harvesting. Nano Energy, 2022, 97, 107175.	16.0	13
6	Fabrication and characterization of nanocomposite based on aramid nanofibers. , 2022, , .		0
7	Laser induced graphene-based out-of-autoclave curing of fiberglass reinforced polymer matrix composites. Composites Science and Technology, 2022, 226, 109529.	7.8	10
8	Cellulose nanocrystal functionalized aramid nanofiber reinforced rubber compounds for tire tread application. Cellulose, 2022, 29, 7735-7749.	4.9	7
9	Laser induced graphene interlaminar reinforcement for tough carbon fiber/epoxy composites. Composites Science and Technology, 2021, 201, 108493.	7.8	34
10	Laser induced graphene for in-situ ballistic impact damage and delamination detection in aramid fiber reinforced composites. Composites Science and Technology, 2021, 202, 108551.	7.8	19
11	Laser induced graphene for in situ damage sensing in aramid fiber reinforced composites. Composites Science and Technology, 2021, 201, 108541.	7.8	18
12	Damage localization in fiberglass-reinforced composites using laser induced graphene. Smart Materials and Structures, 2021, 30, 035006.	3.5	4
13	Artificial neural networks and phenomenological degradation models for fatigue damage tracking and life prediction in laser induced graphene interlayered fiberglass composites. Smart Materials and Structures, 2021, 30, 085010.	3.5	7
14	Fatigue damage tracking and life prediction of fiberglass composites using a laser induced graphene interlayer. Composites Part B: Engineering, 2021, 218, 108935.	12.0	16
15	Transfer printed laser induced graphene strain gauges for embedded sensing in fiberglass composites. Composites Part B: Engineering, 2021, 219, 108932.	12.0	24
16	Dehydrofluorinated PVDF for structural health monitoring in fiber reinforced composites. Composites Science and Technology, 2021, 214, 108982.	7.8	12
17	Improved inter-yarn friction and ballistic impact performance of zinc oxide nanowire coated ultra-high molecular weight polyethylene (UHMWPE). Polymer, 2021, 231, 124125.	3.8	14
18	Isocyanurate transformation induced healing of isocyanurate–oxazolidone polymers. Journal of Applied Polymer Science, 2020, 137, 48698.	2.6	1

#	Article	IF	CITATIONS
19	Nanostructured ZnO Interphase for Carbon Fiber Reinforced Composites with Strain Rate Tailored Interfacial Strength. Advanced Materials Interfaces, 2020, 7, 1901544.	3.7	17
20	Laser induced graphene fibers for multifunctional aramid fiber reinforced composite. Carbon, 2020, 158, 146-156.	10.3	35
21	Laser induced graphene in fiberglass-reinforced composites for strain and damage sensing. Composites Science and Technology, 2020, 199, 108367.	7.8	27
22	Aramid Nanofiber Reinforced Rubber Compounds for the Application of Tire Tread with High Abrasion Resistance and Fuel Saving Efficiency. ACS Applied Polymer Materials, 2020, 2, 4874-4884.	4.4	36
23	3D Printing of a self-healing, high strength, and reprocessable thermoset. Polymer Chemistry, 2020, 11, 6441-6452.	3.9	36
24	Precipitation-Printed High-β Phase Poly(vinylidene fluoride) for Energy Harvesting. ACS Applied Materials & Interfaces, 2020, 12, 58072-58081.	8.0	36
25	Precipitation printing towards diverse materials, mechanical tailoring and functional devices. Additive Manufacturing, 2020, 35, 101358.	3.0	6
26	Aramid Nanofiber Reinforced Polymer Nanocomposites via Amide–Amide Hydrogen Bonding. ACS Applied Polymer Materials, 2020, 2, 2934-2945.	4.4	43
27	Enhanced interfacial strength of hierarchical fiberglass composites through an aramid nanofiber interphase. Composites Science and Technology, 2020, 192, 108109.	7.8	30
28	ZnO Nanostructured Interphase for Multifunctional and Lightweight Glass Fiber Reinforced Composite Materials under Various Loading Conditions. ACS Applied Nano Materials, 2020, 3, 1363-1372.	5.0	17
29	High strength epoxy nanocomposites reinforced by epoxy functionalized aramid nanofibers. Polymer, 2020, 195, 122438.	3.8	46
30	Thermally Stable Poly(vinylidene fluoride) for High-Performance Printable Piezoelectric Devices. ACS Applied Materials & Interfaces, 2020, 12, 21871-21882.	8.0	34
31	Aramid nanofiber interlayer for improved interlaminar properties of carbon fiber/epoxy composites. Composites Part B: Engineering, 2020, 197, 108130.	12.0	33
32	A review of energy harvesting using piezoelectric materials: state-of-the-art a decade later (2008–2018). Smart Materials and Structures, 2019, 28, 113001.	3.5	520
33	Improved Interyarn Friction, Impact Response, and Stab Resistance of Surface Fibrilized Aramid Fabric. Advanced Materials Interfaces, 2019, 6, 1900881.	3.7	13
34	Tailored nanocomposite energy harvesters with high piezoelectric voltage coefficient through controlled nanowire dispersion. Nano Energy, 2019, 60, 620-629.	16.0	12
35	Enhanced interfacial strength of aramid fiber reinforced composites through adsorbed aramid nanofiber coatings. Composites Science and Technology, 2019, 174, 125-133.	7.8	109
36	Vibration Damping Mechanism of Fiber-Reinforced Composites with Integrated Piezoelectric Nanowires. ACS Applied Materials & Interfaces, 2019, 11, 47373-47381.	8.0	9

#	Article	IF	CITATIONS
37	Adsorbed Aramid Nanofiber Interphase for Enhanced Aramid Fiber Reinforced Composites. , 2019, , .		1
38	Electromechanical modeling and experimental verification of a direct write nanocomposite. Smart Materials and Structures, 2019, 28, 045014.	3.5	11
39	Voltage coefficient of a piezoelectric nanocomposite energy harvester: modeling and experimental verification. , 2019, , .		0
40	Energy-harvesting materials for smart fabrics and textiles. MRS Bulletin, 2018, 43, 214-219.	3.5	29
41	Aramid nanofibers for multiscale fiber reinforcement of polymer composites. Composites Science and Technology, 2018, 161, 92-99.	7.8	115
42	Optimal power, power limit and damping of vibration based piezoelectric power harvesters. Smart Materials and Structures, 2018, 27, 075057.	3.5	24
43	Energy Harvesting Performance of Printed Barium Titanate Nanocomposites. , 2018, , .		0
44	Printed Nanocomposite Energy Harvesters with Controlled Alignment of Barium Titanate Nanowires. ACS Applied Materials & Interfaces, 2018, 10, 38359-38367.	8.0	59
45	Novel self-healing CFRP composites with high glass transition temperatures. Composites Science and Technology, 2018, 168, 96-103.	7.8	32
46	In Situ Damage Detection for Fiberâ€Reinforced Composites Using Integrated Zinc Oxide Nanowires. Advanced Functional Materials, 2018, 28, 1802846.	14.9	24
47	Enhanced energy harvesting through nanowire based functionally graded interfaces. Nano Energy, 2018, 52, 171-182.	16.0	21
48	High strength fiber reinforced composites with surface fibrilized aramid fibers. Journal of Applied Physics, 2018, 124, .	2.5	26
49	Electromechanical modeling and experimental verification of a directly printed nanocomposite. , 2018, , .		1
50	Barium Titanate Film Interfaces for Hybrid Composite Energy Harvesters. ACS Applied Materials & Interfaces, 2017, 9, 4057-4065.	8.0	28
51	High service temperature, self-mendable thermosets networked by isocyanurate rings. Polymer, 2017, 114, 249-256.	3.8	12
52	Piezoelectric interfaces enabled energy harvesting and tailored damping in fiber composites. Proceedings of SPIE, 2017, , .	0.8	2
53	Ultra-long vertically aligned lead titanate nanowire arrays for energy harvesting in extreme environments. Nano Energy, 2017, 31, 168-173.	16.0	30
54	Role of ZnO nanowire arrays on the impact response of aramid fabrics. Composites Part B: Engineering, 2017, 127, 222-231.	12.0	47

#	Article	IF	CITATIONS
55	Active photo-thermal self-healing of shape memory polyurethanes. Smart Materials and Structures, 2017, 26, 055003.	3.5	19
56	Isolation of Aramid Nanofibers for High Strength and Toughness Polymer Nanocomposites. ACS Applied Materials & Interfaces, 2017, 9, 11167-11175.	8.0	125
57	Hydrothermal synthesis of tetragonal phase BaTiO3 on carbon fiber with enhanced electromechanical coupling. Journal of Materials Science, 2017, 52, 7893-7906.	3.7	6
58	Biomimetic Nanostructured Interfaces for Hierarchical Composites. Advanced Materials Interfaces, 2016, 3, 1500404.	3.7	26
59	Strain analysis of nanowire interfaces in multiscale composites. Proceedings of SPIE, 2016, , .	0.8	0
60	Energy harvesting from vertically aligned PZT nanowire arrays. Proceedings of SPIE, 2016, , .	0.8	1
61	Self-healing polymers and composites for extreme environments. Journal of Materials Chemistry A, 2016, 4, 17403-17411.	10.3	68
62	Conformal BaTiO <sub>3</sub> Films with High Piezoelectric Coupling through an Optimized Hydrothermal Synthesis. ACS Applied Materials & Interfaces, 2016, 8, 21446-21453.	8.0	24
63	Structure–Property Relationships in Aligned Electrospun Barium Titanate Nanofibers. Journal of the American Ceramic Society, 2016, 99, 3902-3908.	3.8	20
64	Enhanced Interfacial Strength and UV Shielding of Aramid Fiber Composites through ZnO Nanoparticle Sizing. ACS Applied Materials & Interfaces, 2016, 8, 33963-33971.	8.0	134
65	ZnO nanowire interfaces for high strength multifunctional composites with embedded energy harvesting. Energy and Environmental Science, 2016, 9, 634-643.	30.8	83
66	Lead-free 0.5Ba(Zr <sub>0.2</sub> Ti <sub>0.8</sub> )O <sub>3</sub> –0.5(Ba <sub>0.7</sub> Ca <sub>0.3</sub> )TiO< for energy harvesting. Nanoscale, 2016, 8, 5098-5105.	sub <b>ð.ð</b> <td>b&gt;<b>na</b>nowires</td>	b> <b>na</b> nowires
67	Vertically Aligned Lead Titanate Nanowire Arrays for High Temperature Energy Harvesting. , 2015, , .		4
68	Increased interyarn friction through ZnO nanowire arrays grown on aramid fabric. Composites Science and Technology, 2015, 107, 75-81.	7.8	83
69	Morphology-Controlled ZnO Nanowire Arrays for Tailored Hybrid Composites with High Damping. ACS Applied Materials & Interfaces, 2015, 7, 332-339.	8.0	67
70	Adhesive Force Measurement between HOPG and Zinc Oxide as an Indicator for Interfacial Bonding of Carbon Fiber Composites. ACS Applied Materials & Interfaces, 2015, 7, 15380-15387.	8.0	26
71	Highly aligned arrays of high aspect ratio barium titanate nanowires via hydrothermal synthesis. Applied Physics Letters, 2015, 106, .	3.3	21
72	Tailored interyarn friction in aramid fabrics through morphology control of surface grown ZnO nanowires. Composites Part A: Applied Science and Manufacturing, 2015, 76, 326-333.	7.6	34

#	Article	IF	CITATIONS
73	Growth of highly textured PbTiO <sub>3</sub> films on conductive substrate under hydrothermal conditions. Nanotechnology, 2015, 26, 345602.	2.6	5
74	Synthesis of calcium copper titanate (CaCu3Ti4O12) nanowires with insulating SiO2 barrier for low loss high dielectric constant nanocomposites. Nano Energy, 2015, 17, 302-307.	16.0	131
75	Thermally responsive self-healing composites with continuous carbon fiber reinforcement. Composites Science and Technology, 2015, 118, 244-250.	7.8	48
76	Scalable Synthesis of Morphotropic Phase Boundary Lead Zirconium Titanate Nanowires for Energy Harvesting. Advanced Materials, 2014, 26, 7547-7554.	21.0	79
77	Nanowire Arrays: A Low-Frequency Energy Harvester from Ultralong, Vertically Aligned BaTiO3Nanowire Arrays (Adv. Energy Mater. 11/2014). Advanced Energy Materials, 2014, 4, n/a-n/a.	19.5	1
78	Large-scale synthesis of BaxSr1â^'xTiO3 nanowires with controlled stoichiometry. Applied Physics Letters, 2014, 104, .	3.3	34
79	Multifunctional Barium Titanate Coated Carbon Fibers. Advanced Functional Materials, 2014, 24, 6303-6308.	14.9	22
80	Fiber strain sensors from carbon nanotubes self-assembled on aramid fibers. Journal of Intelligent Material Systems and Structures, 2014, 25, 2117-2121.	2.5	14
81	A Lowâ€Frequency Energy Harvester from Ultralong, Vertically Aligned BaTiO <sub>3</sub> Nanowire Arrays. Advanced Energy Materials, 2014, 4, 1301660.	19.5	69
82	Self-Healing: Self-Healing Polyurethanes with Shape Recovery (Adv. Funct. Mater. 33/2014). Advanced Functional Materials, 2014, 24, 5260-5260.	14.9	10
83	Vertically aligned BaTiO <sub>3</sub> nanowire arrays for energy harvesting. Energy and Environmental Science, 2014, 7, 288-296.	30.8	172
84	Controlled synthesis of ultra-long vertically aligned BaTiO <sub>3</sub> nanowire arrays for sensing and energy harvesting applications. Nanotechnology, 2014, 25, 375603.	2.6	51
85	Selfâ€Healing Polyurethanes with Shape Recovery. Advanced Functional Materials, 2014, 24, 5261-5268.	14.9	248
86	Relationship between BaTiO <sub>3</sub> Nanowire Aspect Ratio and the Dielectric Permittivity of Nanocomposites. ACS Applied Materials & Interfaces, 2014, 6, 5450-5455.	8.0	208
87	Toughening mechanism of heterogeneous aliphatic polyurethanes. Polymer, 2014, 55, 2086-2093.	3.8	15
88	Multi-Inclusion modeling of multiphase piezoelectric composites. Composites Part B: Engineering, 2013, 47, 181-189.	12.0	50
89	High-sensitivity accelerometer composed of ultra-long vertically aligned barium titanate nanowire arrays. Nature Communications, 2013, 4, 2682.	12.8	107
90	Hydrothermal growth of textured BaxSr1â^'xTiO3 films composed of nanowires. Nanoscale, 2013, 5, 10901.	5.6	18

6

#	Article	IF	CITATIONS
91	Role of Surface Chemistry in Adhesion between ZnO Nanowires and Carbon Fibers in Hybrid Composites. ACS Applied Materials & Interfaces, 2013, 5, 635-645.	8.0	96
92	Intermolecular interactions dictating adhesion between ZnO and graphite. Carbon, 2013, 63, 517-522.	10.3	11
93	Noncontact and simultaneous measurement of the <i>d</i> 33 and <i>d</i> 31 piezoelectric strain coefficients. Applied Physics Letters, 2013, 102, .	3.3	34
94	Ultra High Energy Density Nanocomposite Capacitors with Fast Discharge Using Ba <sub>0.2</sub> Sr <sub>0.8</sub> TiO <sub>3</sub> Nanowires. Nano Letters, 2013, 13, 1373-1379.	9.1	430
95	Synthesis of High Aspect Ratio BaTiO <sub>3</sub> Nanowires for High Energy Density Nanocomposite Capacitors. Advanced Energy Materials, 2013, 3, 451-456.	19.5	297
96	Vertically Aligned Arrays of BaTiO <sub>3</sub> Nanowires. ACS Applied Materials & Interfaces, 2013, 5, 11894-11899.	8.0	71
97	Barium titanate and barium strontium titanate coated carbon fibers for multifunctional structural capacitors. Journal of Composite Materials, 2013, 47, 1527-1533.	2.4	16
98	Direct measurement of piezoelectric shear coefficient. Journal of Applied Physics, 2013, 113, 214106.	2.5	22
99	Hydrothermal growth of highly textured BaTiO <sub>3</sub> films composed of nanowires. Nanotechnology, 2013, 24, 095602.	2.6	26
100	Relationship between orientation factor of lead zirconate titanate nanowires and dielectric permittivity of nanocomposites. Applied Physics Letters, 2013, 103, .	3.3	41
101	Adhesive Energy of Zinc Oxide and Graphite, Molecular Dynamics and Atomic Force Microscopy Study. Materials Research Society Symposia Proceedings, 2012, 1479, 89-94.	0.1	0
102	Molecular dynamics prediction of interfacial strength and validation through atomic force microscopy. Applied Physics Letters, 2012, 101, .	3.3	14
103	Enhanced Energy Storage in Nanocomposite Capacitors through Aligned PZT Nanowires by Uniaxial Strain Assembly. Advanced Energy Materials, 2012, 2, 469-476.	19.5	233
104	Influence of aspect ratio on effective electromechanical coupling of nanocomposites with lead zirconate titanate nanowire inclusion. Journal of Intelligent Material Systems and Structures, 2011, 22, 1879-1886.	2.5	17
105	Nanocomposites with increased energy density through high aspect ratio PZT nanowires. Nanotechnology, 2011, 22, 015702.	2.6	169
106	Effect of ZnO nanowire morphology on the interfacial strength of nanowire coated carbon fibers. Composites Science and Technology, 2011, 71, 946-954.	7.8	137
107	Carboxyl functionalization of carbon fibers through a grafting reaction that preserves fiber tensile strength. Carbon, 2011, 49, 4246-4255.	10.3	113
108	Interaction of ZnO Nanowires with Carbon Fibers for Hierarchical Composites with High Interfacial Strength. Journal of Solid Mechanics and Materials Engineering, 2010, 4, 1687-1698.	0.5	19

#	Article	IF	CITATIONS
109	Enhanced piezoelectric properties of lead zirconate titanate sol-gel derived ceramics using single crystal PbZr0.52Ti0.48O3 cubes. Journal of Applied Physics, 2010, 108, .	2.5	20
110	Piezoelectric Damping of Resistively Shunted Beams and Optimal Parameters for Maximum Damping. Journal of Vibration and Acoustics, Transactions of the ASME, 2010, 132, .	1.6	21
111	Hydrothermal synthesis of vertically aligned lead zirconate titanate nanowire arrays. Applied Physics Letters, 2009, 95, .	3.3	62
112	Effect of Morphology of ZnO Nanowire Arrays on Interfacial Shear Strength in Carbon Fiber Composites. Materials Research Society Symposia Proceedings, 2009, 1174, 37.	0.1	2
113	Fabrication and Electromechanical Characterization of a Piezoelectric Structural Fiber for Multifunctional Composites. Advanced Functional Materials, 2009, 19, 592-598.	14.9	55
114	Increased Interface Strength in Carbon Fiber Composites through a ZnO Nanowire Interphase. Advanced Functional Materials, 2009, 19, 2654-2660.	14.9	215
115	Structural Effects and Energy Conversion Efficiency of Power Harvesting. Journal of Intelligent Material Systems and Structures, 2009, 20, 505-514.	2.5	64
116	Zinc Oxide Nanowire Interphase for Enhanced Interfacial Strength in Lightweight Polymer Fiber Composites. ACS Applied Materials & Interfaces, 2009, 1, 1827-1833.	8.0	142
117	Optimal parameters and power characteristics of piezoelectric energy harvesters with an <i>RC</i> circuit. Smart Materials and Structures, 2009, 18, 045011.	3.5	52
118	Characterization of multifunctional structural capacitors for embedded energy storage. Journal of Applied Physics, 2009, 106, .	2.5	32
119	Effect of aspect ratio on the electroelastic properties of piezoelectric nanocomposites. Proceedings of SPIE, 2009, , .	0.8	1
120	Concept and model of a piezoelectric structural fiber for multifunctional composites. Composites Science and Technology, 2008, 68, 1911-1918.	7.8	65
121	Energy harvesting through a backpack employing a mechanically amplified piezoelectric stack. Mechanical Systems and Signal Processing, 2008, 22, 721-734.	8.0	241
122	Investigation of an energy harvesting small unmanned air vehicle. Proceedings of SPIE, 2008, , .	0.8	25
123	Modeling of a New Active Eddy Current Vibration Control System. Journal of Dynamic Systems, Measurement and Control, Transactions of the ASME, 2008, 130, .	1.6	19
124	Enhanced active piezoelectric 0-3 nanocomposites fabricated through electrospun nanowires. Journal of Applied Physics, 2008, 103, 124108.	2.5	33
125	Energy harvesting from a backpack instrumented with piezoelectric shoulder straps. Smart Materials and Structures, 2007, 16, 1810-1820.	3.5	312
126	A review of power harvesting using piezoelectric materials (2003–2006). Smart Materials and Structures, 2007, 16, R1-R21.	3.5	2,157

#	Article	IF	CITATIONS
127	A Review of Power Harvesting from Vibration Using Piezoelectric Materials. The Shock and Vibration Digest, 2004, 36, 197-205.	6.2	1,137